Switch to Ca^{2+}-permeable AMPA and reduced NR2B NMDA receptor-mediated neurotransmission at dorsal horn nociceptive synapses during inflammatory pain in the rat

Kristina S. Vikman, Beth K. Rycroft and Macdonald J. Christie

Pain Management Research Institute, Kolling Institute, The University of Sydney at Royal North Shore Hospital, St Leonards NSW 2065, Australia

Glutamate receptor response properties of nociceptive synapses on neurokinin 1 receptor positive ($NK1R^+$) lamina I neurons were determined 3 days after induction of chronic peripheral inflammation with Freund's Complete Adjuvant (CFA). A significant increase in the AMPAR/NMDAR ratio was found during inflammation, which was associated with a significant reduction in the quantal amplitude of NMDAR-mediated synaptic currents. A significant shortening of the quantal AMPA current decay, a greater inward rectification of the AMPAR-mediated eEPSC amplitude and an increased sensitivity to the Ca^{2+}-permeable AMPAR channel blocker 1-naphthylacetyl spermine (NAS) was also observed, indicating an increase in the contribution of Ca^{2+}-permeable AMPARs at this synapse during inflammation. Furthermore the reduced effectiveness of the NR2B-specific antagonist CP-101,606 on NMDAR-mediated eEPSCs together with a decrease in Mg^{2+} sensitivity suggests a down regulation of the highly Mg^{2+}-sensitive and high conductance NR2B subunit at this synapse. These changes in glutamatergic receptor function during inflammation support the selective effectiveness of Ca^{2+}-permeable AMPAR antagonists in inflammatory pain models and may underlie the reported ineffectiveness of NR2B antagonists in spinal antinociception.

(Received 28 September 2007; accepted after revision 12 November 2007; first published online 22 November 2007)
Corresponding author M. J. Christie: Pain Management, University of Sydney at Royal North Shore Hospital, St Leonards 2065 Australia. Email: macc@med.usyd.edu.au

The superficial dorsal horn of the spinal cord is a major area for integration of nociceptive information from the periphery. $NK1R^+$-expressing neurons, which densely populate lamina I (Brown *et al.* 1995; Todd *et al.* 1998), have been associated with the development and maintenance of persistent pain since selective ablation of these neurons results in an almost complete loss of nociceptive behaviour in inflammatory and neuropathic pain models (Mantyh *et al.* 1997; Nichols *et al.* 1999).

Little is known presently about adaptations to glutamatergic neurotransmission or glutamate receptor composition at these synapses during persistent pain states. Alterations in receptor subunit expression and phosphorylation have been reported for AMPAR and NMDAR in the dorsal horn following peripheral noxious stimulation using immunochemical methods (Guo *et al.* 2002, 2004; Nagy *et al.* 2004*a*; Caudle *et al.* 2005). However, the localization of these adaptations to specific populations of dorsal horn neurons, their functional significance and their contribution to the activity of primary afferent synapses is yet to be ascertained during chronic pain. Ultimately changes in glutamatergic function may have consequences for the induction and maintenance of long-term potentiation (LTP) at primary afferent synapses on to dorsal horn neurons which is thought to contribute to hyperalgesia and persistent pain (Ikeda *et al.* 2003, 2006).

In the present study, we investigated glutamate receptor function at nociceptive primary afferent synapses on $NK1R^+$ lamina I neurons after induction of chronic peripheral inflammation with Freund's Complete Adjuvant (CFA). We found an increase in the ratio of AMPAR/NMDAR-mediated components of the primary afferent synapse during inflammation, which was due to reduced amplitude of quantal NMDAR-mediated synaptic currents with no significant change in the amplitude of AMPAR-mediated events. However, the AMPAR component at this synapse showed a shift towards transmission primarily by Ca^{2+}-permeable receptor subtypes whereas the NMDAR component exhibited reduced NR2B subunit contribution and Mg^{2+} sensitivity. These distinct changes in the glutamatergic drive of primary afferent transmission are likely to influence pathological nociceptive sensitivity.

K. S. Vikman and B. K. Rycroft contributed equally to this work.

DOI: 10.1113/jphysiol.2007.145581

Methods

Induction of peripheral inflammation

All experiments were approved by the Joint Royal North Shore Hospital/University of Technology Sydney Animal Care & Ethics Committee which is compliant with the National Health & Medical Research Council's Australian Code of Practice for the Care and Use of Animals for Scientific Purposes and as legislated by the NSW Government. Male and female Sprague–Dawley rats (16–31 days old) were used for all experiments, 74 animals in total. For induction of unilateral peripheral inflammation, animals were anaesthetized with isoflurane (Aerrane; Baxter, Puerto Rico, USA) whereafter 150 μl of CFA (Sigma, Australia) was injected into the plantar surface of the left hind paw. The animals were allowed to recover and were kept for 72 h before being used for electrophysiological experiments, which is within the peak of nociceptive responses associated with this pain model (Iadarola *et al.* 1988; Gu & Huang, 2001). Development of characteristic signs of peripheral inflammation restricted to the hind paw was monitored daily and confirmed in each animal prior to experimentation. The signs included erythema, oedema of the paw and a reduction in weight bearing on the affected paw. Since saline injection into the plantar surface has been shown not to cause any significant changes in mechanical threshold or paw withdrawal latencies (Iadarola *et al.* 1988; Gu & Huang, 2001), naïve rats were used as controls.

Spinal cord slice preparation

Rats were anaesthetized with isoflurane, decapitated and the lumbar region of the spinal cord was removed. Transverse spinal cord slices (350 μm) were cut on a vibratome in an ice-cold solution of the following composition (mM): 100 sucrose, 63 NaCl, 2.5 KCl, 1.2 NaH_2PO_4, 1.2 $MgCl_2$, 2.4 $CaCl_2$, 25 glucose and 2.5 $NaHCO_3$. Slices were maintained at 32°C in a submerged chamber containing physiological saline solution (ACSF) consisting of (mM): 125 NaCl, 2.5 KCl, 1.2 NaH_2PO_4, 1.2 $MgCl_2$, 2.4 $CaCl_2$, 25 glucose and 2.5 $NaHCO_3$ (pH 7.4, osmolarity 305–310 mosmol l^{-1}), which was equilibrated with 95% O_2 and 5% CO_2. The slices were then transferred to a recording chamber and superfused continuously (2 ml min^{-1}) with ACSF. Experiments were performed at 32°C.

Electrophysiology

Lamina I was visualized using infra-red Nomarski optics and neurons were selected for experiments based on size and shape of the cell soma. The mean capacitance of recorded neurons was 36.3 ± 1.4 pF for controls and 35.5 ± 1.3 pF for inflamed animals, as measured from the amplifier's capacitance compensation setting. Neurons with a cell capacitance of ≤ 20 pF were discarded. Whole-cell voltage-clamp recordings (holding potential −74 mV) of synaptic currents were made using a Digidata 1322A and a Multiclamp 700B amplifier (both from Molecular Devices, CA, USA). Patch electrodes with a resistance of 2–4 MΩ were filled with a solution consisting the following (mM): 113 caesium gluconate, 10 EGTA, 10 Hepes, 17.5 CsCl, 8 $NaCl_2$, 3 QX-314, 2 MgATP and 0.3 NaGTP, pH 7.2 (osmolarity, 280–290 mosmol l^{-1}) plus 0.2% biocytin. In some experiments, as indicated in the text, 0.1 mM spermine tetrahydrochloride and 10 mM BAPTA were added to the internal solution. Series resistance (≤ 15 MΩ) was compensated by 80% and continuously monitored during experiments. Liquid junction potentials of −14 mV were corrected for. Recordings were low-pass filtered at 4–6 kHz, sampled at 10 kHz and analysed off-line using Axograph X (Axograph Scientific, Australia). A bipolar tungsten electrode (FHC, ME, USA) was carefully placed in the dorsal root entry zone to ensure stimulation of primary afferent terminals and electrically evoked excitatory postsynaptic currents (eEPSCs) were recorded (0.01 Hz, 2–30 V, 100 μs). To isolate eEPSCs, all experiments were performed in the presence of strychnine (5 μM) and picrotoxin (100 μM) to block glycine- and $GABA_A$-mediated responses. Unless otherwise stated, EPSCs were quantified by averaging a minimum of 20 consecutive responses for each condition. Only evoked currents with a clear first peak were measured and included in the analysis to avoid contamination from polysynaptic events. Recordings of AMPAR/NMDAR ratios were performed at +26 mV. AMPAR-mediated EPSCs were recorded at −74 mV in the presence of the NMDAR antagonist AP5 (100 μM) and the current–voltage relationship was analysed by stepping the holding potential in 20 mV steps up to +46 mV. The response at each voltage step was obtained by averaging a minimum of three consecutive eEPSCs. The rectification index of AMPAR-mediated responses was calculated for each cell by dividing the average peak current at +26 mV by the average peak current obtained at −54 mV. For further study of NMDAR eEPSCs, optimal recordings of glutamatergic eEPSCs were first established at a holding potential of −74 mV, after which the non-NMDAR antagonist CNQX (10 μM) was perfused onto the slices. NMDAR-mediated eEPSCs were studied in normal Mg^{2+} (1.2 mM)-containing ACSF. The current–voltage relationship was examined by recording synaptic currents at a range of holding potentials between −104 mV and +36 mV.

Desynchronization of quantal events underlying the eEPSC was achieved by inclusion of 4–8 mM $SrCl_2$ while reducing $CaCl_2$ to 1 mM in the ACSF solution. Miniature asynchronous evoked postsynaptic currents (aeEPSC) were sampled at 10 s intervals. Data were filtered (2 kHz

low-pass filter) and sampled at 10 kHz for on-line and later off-line analysis (Axograph 4.6; Axon Instruments, Union City, CA, USA). Events above a preset threshold (3.5 S.D.s for AMPA, 2.5 S.D.s for NMDA above baseline noise) were automatically detected by a sliding-template algorithm for a window 100–600 ms post-stimulation to ensure the capture of asynchronous events related to stimulation and then manually checked offline. The first 100 ms post-stimulation in the presence of Sr^{2+} was excluded to reduce the likelihood of including multiquantal, synchronized EPSCs. Events were counted in 500 ms epochs and data pertaining to individual aeEPSC amplitude and 10–90% rise time accumulated. Decay constants for AMPA aeEPSCs were obtained by fitting an exponential function to the averaged aeEPSC current for every cell. Due to the long decay time of the NMDAR, these aeEPSCs could not be fitted to asymptote with an exponential function due to interruption from subsequent aeEPSC therefore tau was measured from the averaged aeEPSC from each individual cell as 63% decrease in the aeEPSC full amplitude.

Immunohistochemistry

At the end of electrophysiological experiments, slices were fixed in 4% paraformaldehyde, 12.5% picric acid in 0.1 M PBS, pH 7.1, for 1 h and then washed in 0.1 M Tris-buffered saline (TBS). For immunohistochemical detection of NK1, slices were washed in 0.1 M PBS, pretreated for 2 h in 5% normal horse serum, 1% bovine serum albumin and 0.3% Triton-X 100 in 0.1 M PBS, followed by incubation with rabbit anti-NK1 (Chemicon, Australia) 1 : 1000–1 : 2000 for 48–72 h at 4°C. For visualization of the primary antibody and biocytin-filled cells, slices were incubated with Alexa 488 donkey anti-rabbit IgG 1 : 200 and Alexa 647–streptavidin conjugate 1 : 500 (both from Invitrogen, Australia) for 2 h at room temperature. All antibodies were diluted in 1% BSA and 0.3% Triton-X 100 in 0.1 M PBS. Slices were then washed in PBS, mounted onto glass slides, air dried for 2 h and cover slipped with Fluoromount-G (ProSciTech, Australia). Images of immunolabelled neurons were obtained using a confocal microscope (Olympus FV-300, Olympus, Australia). Optical sections were collected by sequential scanning with the relevant lasers and NK1 receptor immunopositivity of the recorded neurons was analysed from maximum intensity projections or single optical sections.

Data analysis

Data are expressed as mean ± S.E.M. with n referring to number of cells. Drug effects are presented as percentage inhibition of the baseline response. Statistical differences were assessed using unpaired Student's t test and ANOVA with Bonferroni's multiple comparison test correction, and were plotted using Microsoft Excel and GraphPad Prism software. Statistical significance was set to $P < 0.05$.

Materials

CP-101,606 was a generous gift from Pfizer (Australia), QX-314 chloride was purchased from Alomone Laboratories (Israel), AP5, BAPTA, GYKI 52466, NAS, picrotoxin, spermine tetrahydrochloride and strychnine hydrochloride were all purchased from Sigma (Australia), and CNQX from Tocris Cookson (UK). Stock solutions of all drugs were made in distilled water apart from GYKI 52466 which was dissolved in 0.1 M HCl. Stock solutions were diluted to working concentrations in the extracellular solution immediately before use and applied by superfusion, except for QX-314, BAPTA and spermine tetrahydrochloride which were applied to the internal solution.

Results

Identification of $NK1R^+$ neurons in lamina I

Electrophysiological recordings were obtained from large neurons with preferentially medio-laterally orientated cell soma in the most superficial layer, lamina I, of the spinal dorsal horn. These selection criteria were based on previous studies identifying the morphological characteristics of nociceptive $NK1R^+$ neurons in lamina I (Han *et al.* 1998; Cheunsuang & Morris, 2000). Expression of NK1R in recorded neurons was confirmed *post hoc* by immunohistochemical analysis (Fig. 1*A*). Unless otherwise stated, only $NK1R^+$ neurons were included in analyses; however, the remaining cells selected according to morphological characteristics and capacitance that did not exhibit clear NK1R immunoreactivity, possibly due to cell damage or low expression levels, were representative of the identified $NK1R^+$ population and therefore have also been included for comparison.

Altered synaptic contribution of AMPA and NMDA receptors in $NK1R^+$ neurons during inflammation

Inflammation-induced changes in glutamatergic response properties were first examined by determining the relative contribution of AMPARs and NMDARs (AMPA/NMDAR ratio) to primary afferent synapses of $NK1R^+$ neurons in lamina I. Synaptic currents were recorded at a positive holding potential (+26 mV), where they are composed of both NMDAR- and AMPAR-mediated components (Fig. 1*B*). The AMPAR component was isolated by application of the NMDAR antagonist AP5 (100 μM) and the NMDAR component was then obtained by

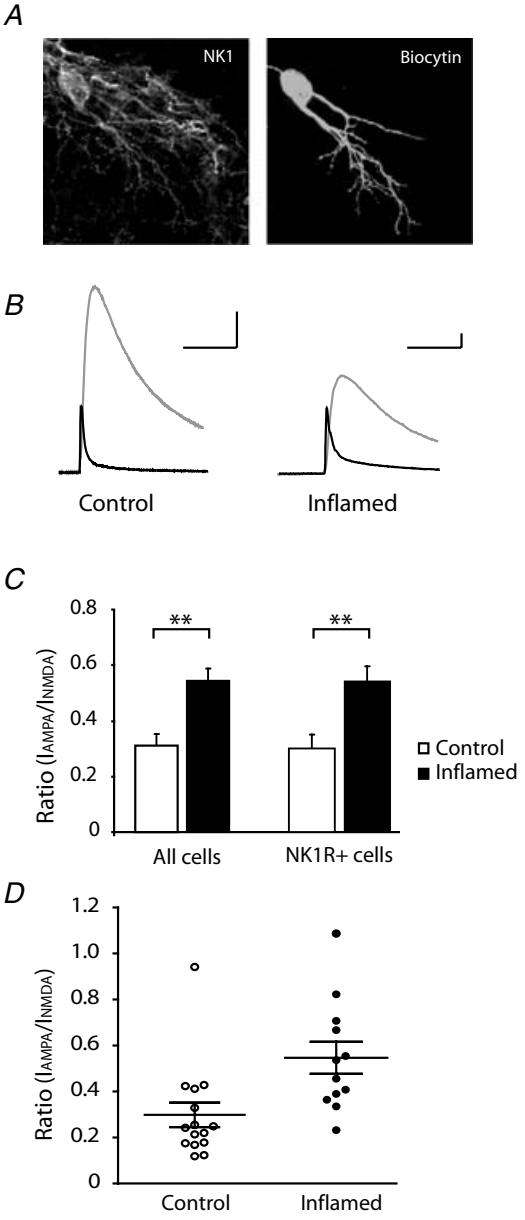

Figure 1. Increased AMPAR/NMDAR ratio of nociceptive synapses in lamina I of the superficial dorsal horn during chronic peripheral inflammation
A, immunohistochemical detection of NK1R expression in a large lamina I neuron filled with biocytin during recording; the dorsal surface is at the top of figure. *B*, averaged traces of synaptic currents recorded at +26 mV from NK1R$^+$ neurons in response to primary afferent stimulation normalized to the AMPAR component (black trace), illustrating the difference between control and inflamed animals in the relative proportion of the NMDAR-mediated component of the synaptic EPSC (grey trace). *C*, histogram showing the increase in the AMPAR/NMDAR ratio in inflamed animals, which was evident in all lamina I neurons recorded as well as the specific population of neurons identified as NK1R$^+$. Data are presented as mean ± S.E.M. *D*, scatter dot plot illustrating the spread in AMPAR/NMDAR ratios in the two experimental groups, where a marked shift towards a higher AMPAR/NMDAR ratio of the total population is observed in the inflamed group. Horizontal bars and error bars indicate the mean ± S.E.M. for each condition. Scale bars in *B* correspond to 25 ms and 0.5 nA. $^{**}P < 0.01$.

subtracting the AMPAR component from the mean pre-drug response (Axograph X). In the presence of AP5 (100 μM), the AMPAR antagonist GYKI 52466 (100 μM) resulted in an almost complete inhibition of the EPSC in both control and inflamed animals (97.2 ± 0.2% for control and 95.6 ± 1.3% for inflamed, $n = 3$ for both groups). The AMPA/NMDAR ratio was significantly increased in cells from inflamed animals compared to controls (0.30 ± 0.05 controls; 0.55 ± 0.07 inflamed, $P < 0.01$; Fig. 1*C* and *D*). An increase in AMPA/NMDAR ratio was observed in all large lamina I cells in the inflamed group, whether or not they were classified as NK1R$^+$ neurons.

No change in quantal AMPAR synaptic amplitude but a reduction in NMDAR amplitude in lamina I NK1R$^+$ neurons during inflammation

An increase in the ratio of AMPA to NMDA receptor-mediated currents can be explained by an increase in the AMPAR-mediated component, a decrease in the NMDAR-mediated component or a mixture of the two. To distinguish between these possibilities we analysed the underlying quantal events that constitute the AMPAR- and NMDAR-mediated eEPSCs. Desynchronizing individual synaptic quantal events with Sr^{2+} (Goda & Stevens, 1994) allowed us to measure quantal amplitude and kinetic data in order to evaluate postsynaptic strength pertaining to the particular synapses under investigation (Oliet *et al.* 1996). Decay kinetics in particular from eEPSCs can be unreliable in the dorsal horn due to the possibility of contamination from polysynaptic events. Quantal events underlying the eEPSC were examined in lamina I NK1R$^+$ neurons by replacing Ca^{2+} in the extracellular recording solution with Sr^{2+} (Fig. 2*A*). Analysis of events revealed that there was no significant difference in amplitude of aeEPSCs between control and inflamed animals (Fig. 2*B*; 25.0 ± 1.4 pA, $n = 13$ in control; 25.9 ± 1.5 pA, $n = 12$ in inflamed, $P > 0.05$). This was also observed in the NK1R$^+$ population (25.3 ± 1.9 pA, $n = 7$ in control; 28.7 ± 1.3 pA, $n = 8$ in inflamed, $P > 0.05$). However, there was a significant decrease in decay time constant of the aeEPSCs (Fig. 2*C*; 1.78 ± 0.1 ms in control and 1.37 ± 0.1 ms in the inflamed group, 1.80 ± 0.1 ms and 1.33 ± 0.1 ms, respectively, for the NK1R$^+$ population, $P < 0.01$), which may be indicative of a change in AMPAR subunit composition such as an increase in Ca^{2+}-permeable AMPARs (Thiagarajan *et al.* 2005). There was also a small but significant reduction in aeEPSC rise time during inflammation from 0.58 ± 0.04 ms in control to 0.48 ± 0.02 ms in the inflamed group (Fig. 2*D*; 0.60 ± 0.03 ms and 0.48 ± 0.03 ms, respectively, for the NK1R$^+$ population, $P < 0.05$).

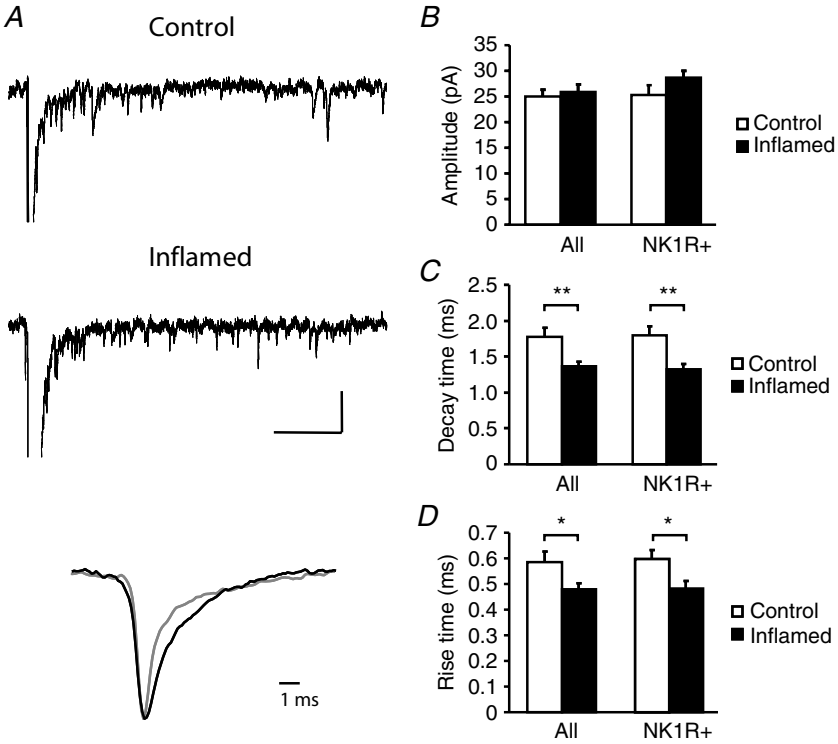

Figure 2. Chronic peripheral inflammation does not change the amplitude but shortens the decay and rise time of asynchronous AMPAR-mediated miniature currents
A, traces of AMPAR-mediated aeEPSCs recorded at −74 mV from a lamina I neuron from a control and inflamed animal, respectively. The lower panel illustrates normalized averaged single currents extracted from the above traces, showing shortening of the decay of the aeEPSC in the inflamed animal (grey) in comparison to control (black). *B–D*, summary histograms displaying mean data ± S.E.M. for aeEPSC amplitude (*B*), decay time (*C*) and rise time (*D*). No significant change in amplitude was observed in neurons from inflamed animals whereas a significant reduction in both decay time and rise time was evident in all lamina I neurons recorded as well as the population of neurons identified as $NK1R^+$. Scale bars in *A* correspond to 100 ms and 50 pA. $^*P < 0.05$, $^{**}P < 0.01$.

In contrast to the lack of effect of inflammation on the amplitude of AMPAR-mediated aeEPSCs, the mean amplitude of NMDAR-mediated aeEPSCs in all cells was reduced during inflammation (Fig. 3*A* and *B*; 34.4 ± 3.6 pA, $n = 15$, in control and 25.4 ± 1.7 pA, $n = 17$, in the inflamed group: $P < 0.05$) as well as in the $NK1R^+$ population (36.3 ± 5.9 pA, $n = 5$, and 20.1 ± 0.9 pA, $n = 4$, respectively: $P < 0.05$). The rise time of the NMDAR-mediated aeEPSC was also affected, being significantly shorter in the inflamed group (2.0 ± 0.08 ms) when compared to control (Fig. 3*C*; 2.4 ± 0.1 ms, $P < 0.05$). A similar trend was also observed in the $NK1R^+$ population (2.3 ± 0.3 ms in control and 1.8 ± 0.09 ms in the inflamed group). Interestingly, estimation of the NMDAR-mediated aeEPSC decay appeared to be slightly but significantly slower during inflammation. Measurements of tau as a 63% decrease of the full aeEPSC amplitude were 35.5 ± 0.7 ms in control

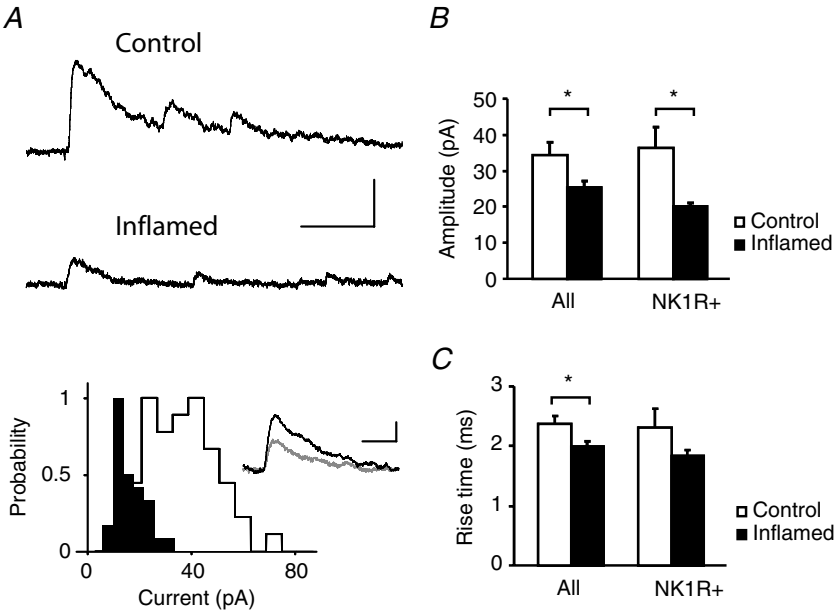

Figure 3. Chronic peripheral inflammation decreases the amplitude and shortens the rise time of asynchronous NMDAR-mediated miniature currents
A, traces of NMDAR-mediated aeEPSCs recorded at +26 mV from lamina I neurons from a control and inflamed animal, respectively. The histogram displays the distribution of individual amplitudes for the same neurons (open bars, control animal; filled bars, inflamed animal), and the inset illustrates the average current from the same cells (control, black trace; inflamed, grey trace). *B* and *C*, summary histograms displaying mean data ± S.E.M. for aeEPSC amplitude (*B*) and rise time (*C*) for both experimental groups. A significant reduction in both amplitude and rise time was evident in all lamina I neurons recorded as well as the population of neurons identified as $NK1R^+$. Upper scale bars in *A* correspond to 100 ms and 100 pA, and lower scale bars to 20 ms and 20 pA, $^*P < 0.05$.

and 39.7 ± 1.5 in the inflamed group (34.3 ± 1.2 ms and 39.2 ± 1.2 ms, respectively, for the NK1R$^+$ population, $P < 0.05$).

Increased contribution of Ca^{2+}-permeable AMPAR subunits to primary afferent eEPSCs in NK1R$^+$ lamina I neurons during inflammation

The physiological properties of AMPARs are determined by its subunit composition (for review, see Dingledine *et al.* 1999). The presence of GluR2 abolishes permeation by Ca^{2+}, hence receptors lacking this subunit are referred to as Ca^{2+}-permeable AMPARs. One characteristic of Ca^{2+}-permeable AMPARs is an inwardly rectifying current–voltage (*I–V*) relationship, which is due to blockade by intracellular polyamines (Bowie & Mayer, 1995). *I–V* relationships of primary afferent eEPSCs were studied in NK1R$^+$ lamina I neurons in the presence of AP5 (100 μM) with the addition of 0.1 mM spermine to the intracellular solution to compensate for a possible loss of endogenous polyamines from dialysis during recording. As shown in Fig. 4*A*; *I–V* curves from NK1R$^+$ neurons in control animals showed weak rectification at positive potentials whereas a profound inward rectification at positive potentials was observed in inflamed animals. The rectification index of NK1R$^+$ lamina I neurons from control animals ranged from 0.48 to 1.04 ($n = 14$), indicating that there is considerable variation in the contribution of Ca^{2+}-permeable AMPARs at primary afferent synapses onto different lamina I cells under control conditions (Fig. 4*B*). By contrast, the rectification index in inflamed animals ranged from 0.33 to 0.60 ($n = 14$), which was significantly lower than in controls (0.62 ± 0.04 in control *versus* 0.42 ± 0.03 in inflamed, $P < 0.01$) (Fig. 4*B* and *C*). This suggests increased contribution of Ca^{2+}-permeable AMPARs to the primary afferent synaptic responses of NK1R$^+$ lamina I neurons during inflammation.

To verify that the enhanced rectification observed in inflamed animals was due to block of outward currents by

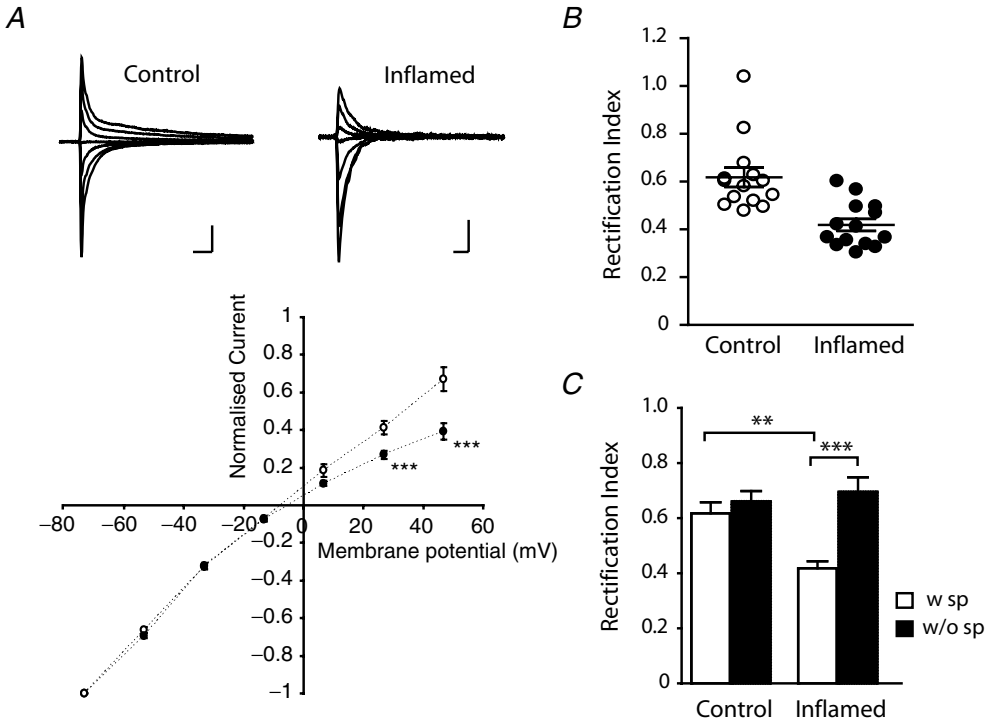

Figure 4. Peripheral inflammation causes a shift in the *I–V* relationship of primary afferent-evoked AMPAR-mediated currents at nociceptive synapses in lamina I

A, upper panel illustrates traces of AMPAR-mediated eEPSCs recorded at different holding potentials (as plotted in lower panel) from an NK1R$^+$ neuron of a control and inflamed animal, respectively. The diagram in the lower panel shows that the rectification at positive potentials of the *I–V* relationship of NK1R$^+$ neurons is significantly enhanced in inflamed animals. *B*, scatter plot illustrating the spread in rectification index (I_{+26mV}/I_{-54mV}) of recorded neurons from the two experimental groups, with a marked shift towards lower rectification index in the inflamed group ($P < 0.001$, ANOVA). Horizontal bars and error bars indicate the mean ± S.E.M. for each condition. *C*, the significant reduction in mean rectification index of the inflamed group was due to blockade by intracellular spermine (open bars) and the reduction was abolished in the absence of spermine (filled bars) in the intracellular recording solution. Data are presented as mean ± S.E.M. Scale bars in *A* correspond to 10 ms and 1 nA. $^{**}P < 0.01$, $^{***}P < 0.001$.

intracellular polyamines, we examined the rectification index without the addition of exogenous spermine to the intracellular solution (Fig. 4*C*). There was only a small change in the rectification index of control $NK1R^+$ lamina I neurons in the absence of intracellular spermine (from 0.62 ± 0.04 to 0.66 ± 0.03, $n = 19$) but the reduction in rectification index was abolished in the inflamed group (from 0.42 ± 0.03 to 0.69 ± 0.05, $n = 13$, $P < 0.001$, ANOVA), which confirms an increased contribution of Ca^{2+}-permeable AMPARs during inflammation.

Another characteristic of Ca^{2+}-permeable AMPARs is sensitivity to blockade by extracellularly applied polyamines, such as Joro spider toxin (Blaschke *et al.* 1993). To determine the sensitivity of AMPAR-mediated eEPSCs in lamina I $NK1R^+$ cells to extracellular polyamines we used a synthetic analogue of Joro spider toxin, NAS (Koike *et al.* 1997). NAS (100 μM) inhibited the eEPSC amplitude in control animals by $26.3 \pm 1.9\%$ ($n = 17$) whereas inflamed animals were significantly more sensitive to NAS, being inhibited by $46.6 \pm 3.1\%$ ($n = 15$; $P < 0.01$, Fig. 5*A–C*), providing further confirmation of increased contribution of Ca^{2+}-permeable AMPARs to synaptic currents during inflammation.

Reduced NMDAR contribution to eEPSCs is not due to enhanced AMPAR-mediated Ca^{2+} entry

It has previously been shown that Ca^{2+} influx through Ca^{2+}-permeable AMPARs can desensitize neighbouring NMDARs in dorsal horn neurons (Kyrozis *et al.* 1995), which may explain the observed reduction in contribution of NMDARs to the eEPSC during inflammation. A separate series of experiments was performed in which the AMPAR/NMDAR ratio was recorded in the presence of a high concentration of the Ca^{2+} chelator BAPTA (10 mM) in the intracellular solution to buffer intracellular Ca^{2+} and thereby diminish Ca^{2+}-dependent desensitization of the NMDAR (Tong *et al.* 1995). Fast chelation of intracellular Ca^{2+} by BAPTA had no effect on the AMPAR/NMDAR ratio during inflammation, which again was significantly higher in inflamed animals (0.64 ± 0.7, $n = 5$), than in controls (0.38 ± 0.05, $n = 7$, $P < 0.05$). This suggests that Ca^{2+}-dependent desensitization of NMDARs does not account for the decrease in NMDAR contribution during inflammation.

Inflammation-induced changes in NMDAR properties of nociceptive synapses in lamina I

The observed reduction in contribution of NMDARs to primary afferent eEPSCs onto $NK1R^+$ neurons in lamina I during inflammation could be due to selective loss or redistribution of NMDAR subunits. We therefore next considered whether persistent inflammation causes

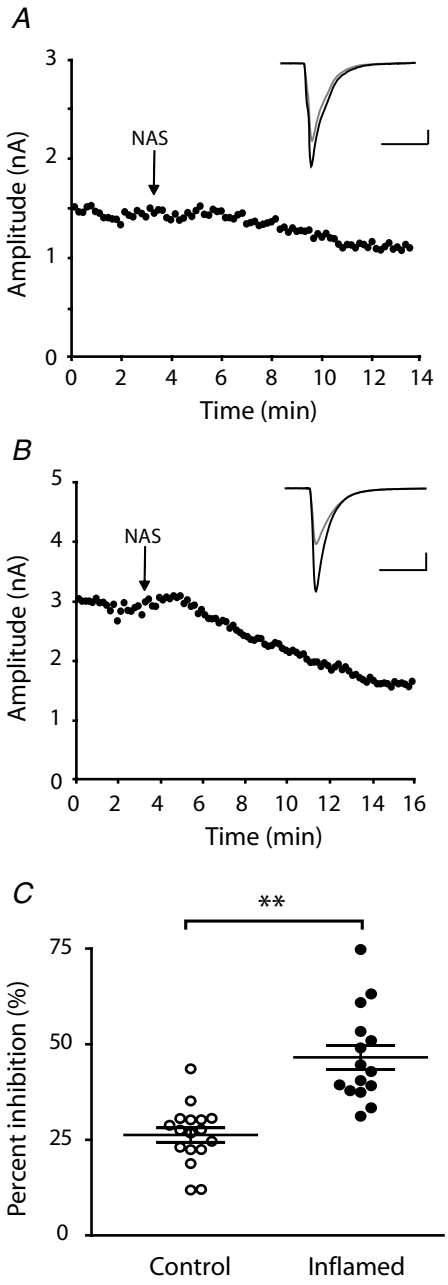

Figure 5. Increased sensitivity of primary afferent-evoked AMPAR-mediated currents to blockade by extracellular polyamines during chronic peripheral inflammation
A and *B*, examples of recordings from individual $NK1R^+$ neurons from a control (*A*) and inflamed animal (*B*), illustrating that superfusion of the synthetic Joro spider toxin analogue NAS (100 μM) (application commenced at the arrow) during recording of AMPAR-mediated eEPSCs resulted in a minor reduction in amplitude in control animals but had a marked effect on eEPSC amplitude in inflamed animals. Insets correspond to single eEPSCs recorded from the cell, at baseline prior to NAS application (black trace) and after the NAS effect had stabilized (grey trace). *C*, scatter plot illustrating the spread in inhibitory effect of NAS on AMPAR-mediated eEPSC amplitude in the two experimental groups. Horizontal bars and error bars indicate the mean ± S.E.M. for each condition. Chronic peripheral inflammation caused a significant increase in sensitivity of synaptic AMPAR-mediated currents to inhibition by NAS. Scale bars in *A* correspond to 10 ms and 0.2 nA and in *B* to 10 ms and 0.5 nA. $^{**}P < 0.01$.

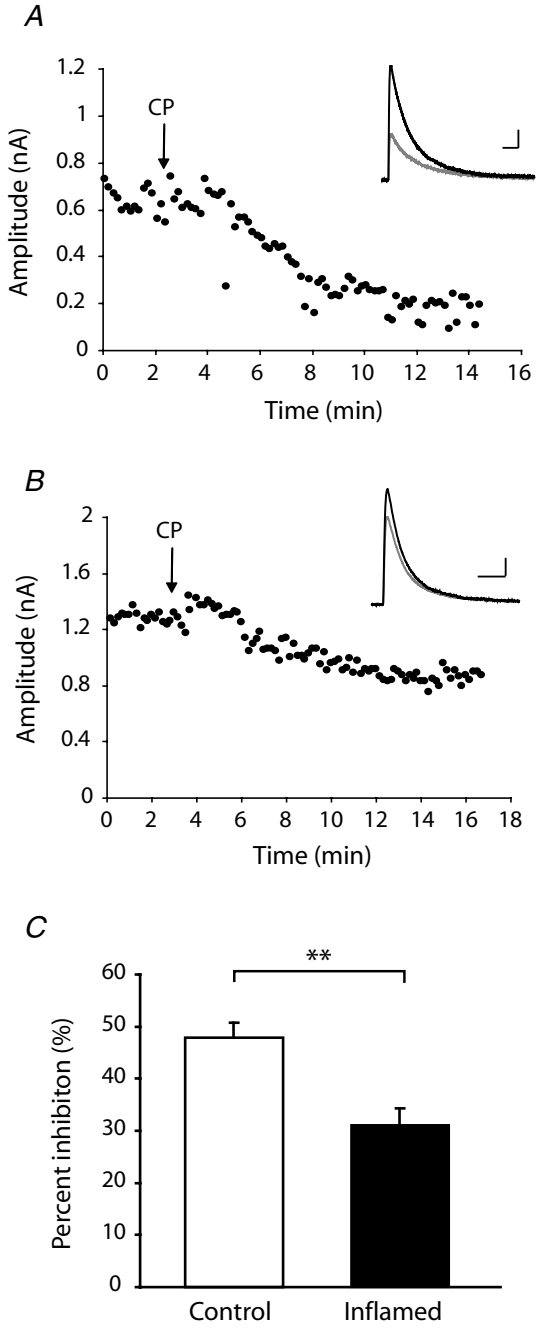

Figure 6. Reduced contribution of NR2B-containing NMDARs to primary afferent-evoked EPSCs at nociceptive synapses in lamina I during chronic peripheral inflammation
A and *B*, examples of recordings from individual NK1R$^+$ neurons from a control (*A*) and inflamed animal (*B*), illustrating that superfusion of the NR2B inhibitor CP-101,606 (5 μM) (application commenced at the arrow) during recording of NMDAR-mediated EPSCs at +26 mV had a smaller effect on amplitude in inflamed animals than in control. Insets correspond to single eEPSCs recorded from the cell, at baseline prior to CP application (black trace) and after the effect of CP has stabilized (grey trace). *C*, summary histogram showing that the inhibitory effect of CP was significantly reduced in animals with peripheral inflammation. Data are presented as mean ± S.E.M. Scale bars in *A* correspond to 100 ms and 100 pA and in *B* to 50 ms and 200 pA. $^{**}P < 0.01$.

changes to the NMDAR response properties of nociceptive synapses. As the NR2B subunit is highly localized within the superficial dorsal horn (Nagy *et al.* 2004*b*), its contribution to the NMDAR-mediated eEPSC at +26 mV to release Mg^{2+} block was investigated using the non-competitive NR2B antagonist CP-101,606 (5 μM) (Brimecombe *et al.* 1997) in the presence of CNQX (10 μM) (Fig. 6*A* and *B*). In control animals, CP-101,606 reduced the amplitude of the NMDAR-mediated EPSC by 47.8 ± 3.0% ($n = 10$) whereas the effect in inflamed animals was significantly smaller (31.1 ± 3.2%, $n = 7$, $P < 0.01$) (Fig. 6*C*), indicating that the contribution of NR2B-containing receptors to the primary afferent EPSC onto NK1R$^+$ neurons in lamina I is reduced during inflammation.

NMDAR subunits exhibit different Mg^{2+} sensitivity which may provide additional information as to subunit changes during inflammation. *I–V* curves from NK1R$^+$ lamina I neurons in both control ($n = 12$) and inflamed ($n = 11$) animals showed a typical negative slope conductance due to voltage-dependent block of NMDAR channels by Mg^{2+} (Fig. 7*A*). When *I–V* relationships for each cell were normalized to the maximum outward current at +36 mV, significantly reduced rectification at negative potentials was observed in inflamed animals ($P < 0.01$, ANOVA) (Fig. 7*B*). Reduced rectification suggests a decrease in the Mg^{2+} sensitivity of the NMDAR-mediated EPSC during inflammation.

Discussion

The present study demonstrates that chronic peripheral inflammation is associated with profound changes in the contribution of distinct glutamatergic receptor subtypes to nociceptive synaptic transmission in the superficial spinal dorsal horn. Although there was an increase in AMPAR/NMDAR ratio during inflammation, this was not associated with an increase in synaptic quantal amplitude of AMPAR-mediated currents but rather due to a decrease in the quantal amplitude of the NMDAR component. However, redistribution of AMPAR subunits occurred with an increased relative contribution of Ca^{2+}-permeable AMPARs to the synaptic response, as indicated by a shortening of the quantal aeEPSC decay, increased polyamine-mediated rectification of the AMPA-mediated eEPSC and increased sensitivity to the Ca^{2+}-permeable AMPAR blocker NAS. Reduction of the NMDAR quantal amplitude was attributed to a down-regulation of the highly Mg^{2+}-sensitive NR2B subunit. This was suggested by a decrease in the inhibition of NMDAR-mediated eEPSCs by the selective NR2B antagonist CP-101,606 and further supported by a reduction in the Mg^{2+} sensitivity of these currents in inflamed animals. We previously reported (Rycroft *et al.* 2007) that the same inflammatory pain model did not affect the paired-pulse

ratio at this synapse, suggesting that the alterations in AMPAR and NMDAR function observed here must relate to a change in postsynaptic glutamatergic function rather than presynaptic release probability. Whilst we have not determined whether these adaptations are exclusively localized in the neuronal population investigated in this study, the changes we have observed in lamina I NK1 expressing cells are likely to be of importance to nociceptive signalling in the dorsal horn.

The relevance of Ca^{2+}-permeable AMPARs for inflammatory pain

The present results suggest that increased contribution of Ca^{2+}-permeable AMPARs to nociceptive primary afferent synapses may contribute to enhanced pain responsiveness at the peak of inflammatory hyperalgesia, 3 days after CFA injection. This is consistent with GluR2 lacking Ca^{2+}-permeable AMPARs being strongly implicated in nociceptive plasticity and inflammatory pain hypersensitivity (Hartmann *et al.* 2004). Ca^{2+}-permeable AMPARs are assembled as a combination of GluR1, 3 and 4 and are associated with a larger conductance and faster decay kinetics (Thiagarajan *et al.* 2005). GluR1 is the most abundant subunit in the superficial dorsal horn with a predominant localization to nociceptive synapses (Nagy *et al.* 2004*a*) and the presence of Ca^{2+}-permeable AMPARs has been demonstrated in specific subpopulations of neurons in the dorsal horn, including $NK1R^+$ neurons in lamina I (Tong & MacDermott, 2006). Recently, GluR2 expression was identified in the vast majority of all AMPAR immunoreactive sites in the dorsal horn (Nagy *et al.* 2004*a*), suggesting a mixture of Ca^{2+}-permeable and -impermeable AMPARs occurs throughout this region. A varying degree of inward rectification of the AMPAR-mediated EPSCs in control animals was observed in the present study confirming the presence of both types of AMPARs at nociceptive synapses on $NK1R^+$ lamina I neurons.

The increased contribution of Ca^{2+}-permeable AMPARs without any evidence for a change in the quantal synaptic AMPAR current during chronic inflammation suggests that a switch in receptor subtype may have occurred at the nociceptive synapses of lamina I $NK1R^+$ neurons. By contrast, a change in the quantal amplitude of the aeEPSC might have been expected if additional insertion of the larger conductance Ca^{2+}-permeable AMPARs had occurred without loss of Ca^{2+}-impermeable AMPARs. Similarly, Plant *et al.* (2006) reported an increased contribution of Ca^{2+}-permeable AMPARs during induction of LTP that was associated with the increased synaptic strength at the Schaffer collateral synapse. Subsequently, during maintenance of LTP the contribution of Ca^{2+}-permeable AMPARs abated without loss of synaptic strength, as Ca^{2+}-permeable AMPARs switched to impermeable AMPARs at potentiated synapses.

Another possible explanation for a reduction in the NMDAR component with no marked change in the size of quantal AMPARs is the unsilencing of synapses during inflammation. Reversion of pure NMDAR silent synapses to active synapses containing both AMPA and NMDARs has previously been implicated in synaptic plasticity

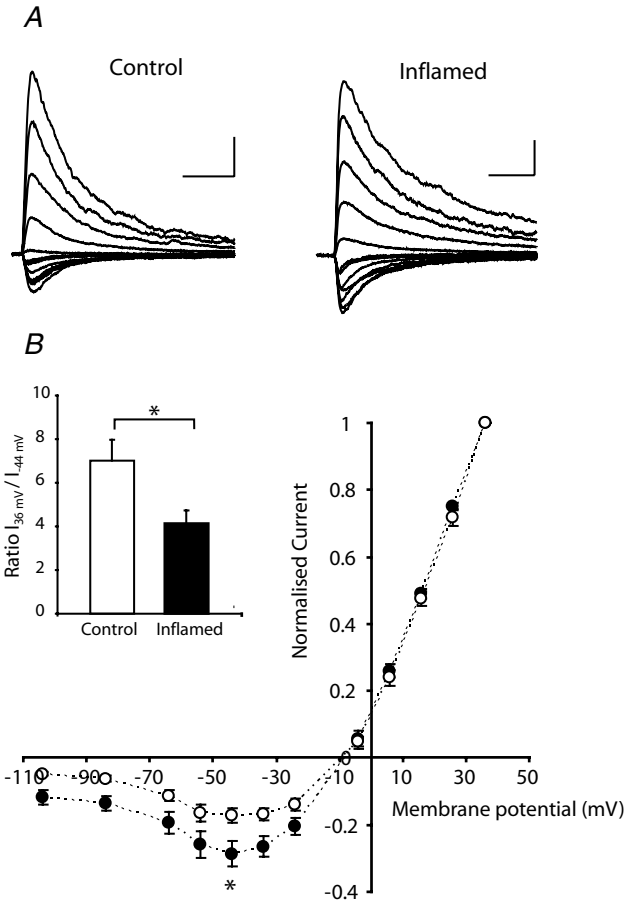

Figure 7. Primary afferent-evoked NMDAR-mediated synaptic currents show reduced Mg^{2+} sensitivity during chronic peripheral inflammation
A, traces of NMDAR-mediated eEPSCs recorded at different holding potentials (as plotted in lower panel) from an $NK1R^+$ lamina I neuron of a control and inflamed animal showing a typical negative slope conductance due to voltage-dependent block by Mg^{2+}. Scale bars correspond to 50 ms and 0.3 nA for control and 50 ms and 0.5 nA for inflamed. *B*, the diagram illustrates the mean *I–V* relationship of NMDAR-mediated eEPSCs for each experimental group, normalized to the maximum outward current at +36 mV, and the significantly reduced rectification at negative potentials in the inflamed group ($P < 0.01$, ANOVA). Inset shows a summary histogram of un-normalized data, comparing the mean ratio of the maximum outward current (at +36 mV) and the maximum inward current (at −44 mV) for each experimental group. The ratio is significantly smaller in the inflamed group, which confirms a reduced Mg^{2+} sensitivity of NMDAR-mediated eEPSCs at negative potentials during peripheral inflammation. $^*P < 0.05$.

(Isaac, 2003; Franks & Isaacson, 2005). Silent synapses are present in the dorsal horn and have been implicated in nociception (Bardoni *et al.* 1998; Li & Zhuo, 1998; Jung *et al.* 2005). However, their relevance for pain transmission is hampered by their predominant expression being during the first two postnatal weeks (Li & Zhuo, 1998) and the lack of evidence for their presence in adult animals (Baba *et al.* 2000). Given that animals used in this study were older than 2 weeks, we consider that unsilencing of synapses is unlikely to contribute greatly to the observed differences in glutamatergic drive reported here.

Interactions of auxillary proteins with AMPA and NMDARs could also have contributed to the changes observed during inflammation. Soto *et al.* (2007) recently demonstrated that interaction of Ca^{2+}-permeable AMPARs with the auxillary protein Stargazin reduced block by intracellular polyamines and therefore inwardly rectifying characteristics. As an alternative mechanism it is possible that inflammation reduces expression of Stargazin resulting in an increased sensitivity of Ca^{2+}-permeable AMPARs to polyamines and exhibiting a greater inward rectification at positive potentials. However, our observation of the increased effect of Ca^{2+}-permeable AMPAR-selective antagonist NAS and shortening of the aeEPSC decay during inflammation still favour the interpretation that the contribution of Ca^{2+}-permeable AMPARs at primary afferent synapses is increased during inflammation. Nonetheless, it would be interesting to investigate the expression of Stargazin in the dorsal horn during inflammation.

While NMDAR activation and synergistic interaction with other pathways for elevation of $[Ca^{2+}]_i$ has been shown to be necessary for induction of LTP in lamina I neurons (Ikeda *et al.* 2006), calcium influx through Ca^{2+}-permeable AMPARs may also contribute to this process as has been shown in the hippocampus (Plant *et al.* 2006). It has become widely accepted that LTP is associated with rapid incorporation of AMPARs into synapses, which consequently enhances the synaptic strength (for review, see Collingridge *et al.* 2004). However, an exchange of receptor subtypes in the synaptic pool, as was first described in cerebellar stellate cells (Liu & Cull-Candy, 2000), is also suggested as a mechanism for regulation of synaptic efficacy in addition to the traditional view of changes in AMPAR numbers/receptor insertion. Furthermore, specific AMPAR redistribution with a switch to Ca^{2+}-permeable receptors has recently been described for long-lasting plasticity in the brain (Bellone & Luscher, 2006).

Inflammation induced changes in NMDAR properties of nociceptive synapses

The increased AMPAR/NMDAR ratio observed during inflammation can be explained by a change in the NMDAR component as the quantal amplitude of the Sr^{2+}-induced asynchronous NMDAR-mediated currents was reduced. In addition to marked changes in contribution of Ca^{2+}-permeable AMPARs, we also observed distinct modifications/reduction of the NMDAR-mediated responses of nociceptive synapses of $NK1R^+$ lamina I neurons during chronic inflammation. The reduction in the NMDAR quantal amplitude during inflammation could be due to down-regulation of the high conductance NR2B subunit in lamina I, which would be consistent with the observed reduced effect of the NR2B-specific antagonist CP-101,606. Reports describing phosphorylation of NR2B, a priming mechanism for internalization (Guo *et al.* 2002, 2004), as well as reduced expression of NR2B following chronic peripheral inflammation (Caudle *et al.* 2005) are consistent with this possibility. Alternatively or additionally, reduced NMDAR quantal amplitude may have resulted from a subunit-specific switch in NMDAR subtypes. A proportional up-regulation of the lower conductance NR2D or NR3A subunits (Wyllie *et al.* 1996; Das *et al.* 1998) that also exist in the superficial dorsal horn (Tölle *et al.* 1993; Ciabarra *et al.* 1995) would be expected to produce a smaller quantal NMDAR current. The reduced sensitivity of NMDAR-mediated EPSCs to Mg^{2+}-dependent rectification at negative potentials in inflamed animals is also consistent with this possibility as both NR2D and NR3A subunits exhibit reduced Mg^{2+} sensitivity in comparison to the NR2B subunit (Monyer *et al.* 1994; Sasaki *et al.* 2002). Furthermore, NR2D-containing NMDARs exhibit slower inactivation kinetics (Monyer *et al.* 1994; Wyllie *et al.* 1998), which may underlie the slight slowing of the estimated decay of the NMDA-mediated quantal current observed here. However, studies have yet to prove that the NR2D subunit occurs synaptically favouring a more extrasynaptic role (Brickley *et al.* 2003) and without specific antagonists for the NR2D or NR3A subunits up-regulation of their function is hard to assess.

Although at positive holding potentials the quantal amplitude of the NMDAR-mediated eEPSC was reduced during inflammation, it is likely that at negative membrane potentials (less than -20 mV) and physiological Mg^{2+} concentrations, more current will be mediated by the less Mg^{2+}-sensitive NMDARs. Thus, we predict that NMDAR-mediated signalling in the dorsal horn may in fact be increased during inflammation consistent with the observations of Guo & Huang (2001). Furthermore this increase in NMDAR-mediated transmission and subsequent calcium influx during inflammation could contribute to enhancement of LTP, an NMDAR-dependent process in lamina I of the dorsal horn (Ikeda *et al.* 2003, 2006). Indeed removing the Mg^{2+} block of NMDARs has been shown to enhance LTP in the nucleus accumbens (Schramm *et al.* 2002). In addition, changing

NMDAR Mg^{2+} sensitivity will have vast implications for other dependent integrative synaptic processes such as coincidence detection and synaptic refinement (Rudhard *et al.* 2003).

Implications

These findings present evidence of specific adaptations in excitatory response properties underlying the maintenance of inflammatory pain hypersensitivity at nociceptive synapses in lamina I of the spinal dorsal horn beyond the initial period of synaptic plasticity. Taken together, our results establish emergence of Ca^{2+}-permeable AMPAR-mediated transmission at nociceptive synapses in lamina I during chronic peripheral inflammation, implicating the physiological relevance of Ca^{2+}-permeable AMPARs for long-lasting inflammatory pain hypersensitivity as previously suggested (Hartmann *et al.* 2004).

Studies of selective AMPAR and NMDAR antagonists in experimental pain models have shown discrepancies in their efficacy for blocking hyperalgesia, depending on the type and duration of the pain condition, suggesting that time- and injury-specific changes in glutamate receptor subtypes occur in spinal pain pathways (Bleakman *et al.* 2006). This complexity emphasizes the importance of elucidating the adaptive changes occurring in nociceptive synapses in the spinal dorsal horn in order to better optimize treatment regimes for different pain conditions. Our finding of an increased contribution of Ca^{2+}-permeable AMPARs during inflammation is consistent with the reported selective effectiveness of Ca^{2+}-permeable AMPAR antagonists in inflammatory pain models (Sorkin *et al.* 2001; Hartmann *et al.* 2004). In addition, our results suggest that down- regulation of NR2B subunit contribution to NMDAR function during inflammation may underlie the ineffectiveness of NR2B antagonists in spinal antinociception (Chizh *et al.* 2001). If, as our results suggest, NR2D or NR3A subunits contribute more substantially to NMDAR function during chronic inflammation these subunits may provide a more amenable pharmacological target for chronic inflammatory pain relief.

References

Baba H, Doubell TP, Moore KA & Woolf CJ (2000). Silent NMDA receptor-mediated synapses are developmentally regulated in the dorsal horn of the rat spinal cord. *J Neurophysiol* **83**, 955–962.

Bardoni R, Magherini PC & MacDermott AB (1998). NMDA EPSCs at glutamatergic synapses in the spinal cord dorsal horn of the postnatal rat. *J Neurosci* **18**, 6558–6567.

Bellone C & Luscher C (2006). Cocaine triggered AMPA receptor redistribution is reversed in vivo by mGluR-dependent long-term depression. *Nat Neurosci* **9**, 636–641.

Blaschke M, Keller BU, Rivosecchi R, Hollmann M, Heinemann S & Konnerth A (1993). A single amino acid determines the subunit-specific spider toxin block of α-amino-3-hydroxy-5-methylisoxazole-4-propionate/kainate receptor channels. *Proc Natl Acad Sci U S A* **90**, 6528–6532.

Bleakman D, Alt A & Nisenbaum ES (2006). Glutamate receptors and pain. *Semin Cell Dev Biol* **17**, 592–604.

Bowie D & Mayer ML (1995). Inward rectification of both AMPA and kainate subtype glutamate receptors generated by polyamine-mediated ion channel block. *Neuron* **15**, 453–462.

Brickley SG, Misra C, Mok MH, Mishina M & Cull-Candy SG (2003). NR2B and NR2D subunits coassemble in cerebellar Golgi cells to form a distinct NMDA receptor subtype restricted to extrasynaptic sites. *J Neurosci* **23**, 4958–4966.

Brimecombe JC, Boeckman FA & Aizenman E (1997). Functional consequences of NR2 subunit composition in single recombinant N-methyl-D-aspartate receptors. *Proc Natl Acad Sci U S A* **94**, 11019–11024.

Brown JL, Liu H, Maggio JE, Vigna SR, Mantyh PW & Basbaum AI (1995). Morphological characterization of substance P receptor-immunoreactive neurons in the rat spinal cord and trigeminal nucleus caudalis. *J Comp Neurol* **356**, 327–344.

Caudle RM, Perez FM, Del Valle-Pinero AY & Iadarola MJ (2005). Spinal cord NR1 serine phosphorylation and NR2B subunit suppression following peripheral inflammation. *Mol Pain* **1**, 25.

Cheunsuang O & Morris R (2000). Spinal lamina I neurons that express neurokinin I receptors: morphological analysis. *Neuroscience* **97**, 335–345.

Chizh BA, Headley PM & Tzschentke TM (2001). NMDA receptor antagonists as analgesics: focus on the NR2B subtype. *Trends Pharmacol Sci* **22**, 636–642.

Ciabarra AM, Sullivan JM, Gahn LG, Pecht G, Heinemann S & Sevarino KA (1995). Cloning and characterization of χ-1: a developmentally regulated member of a novel class of the ionotropic glutamate receptor family. *J Neurosci* **15**, 6498–6508.

Collingridge GL, Isaac JT & Wang YT (2004). Receptor trafficking and synaptic plasticity. *Nat Rev Neurosci* **5**, 952–962.

Das S, Sasaki YF, Rothe T, Premkumar LS, Takasu M, Crandall JE, Dikkes P, Conner DA, Rayudu PV, Cheung W, Chen HS, Lipton SA & Nakanishi N (1998). Increased NMDA current and spine density in mice lacking the NMDA receptor subunit NR3A. *Nature* **393**, 377–381.

Dingledine R, Borges K, Bowie D & Traynelis SF (1999). The glutamate receptor ion channels. *Pharmacol Rev* **51**, 7–61.

Franks KM & Isaacson JS (2005). Synapse-specific downregulation of NMDA receptors by early experience: a critical period for plasticity of sensory input to olfactory cortex. *Neuron* **47**, 101–114.

Goda Y & Stevens CF (1994). Two components of transmitter release at a central synapse. *Proc Natl Acad Sci U S A* **91**, 12942–12946.

Gu Y & Huang LY (2001). Gabapentin actions on N-methyl-D-aspartate receptor channels are protein kinase C-dependent. *Pain* **93**, 85–92.

Guo H & Huang LY (2001). Alteration in the voltage dependence of NMDA receptor channels in rat dorsal horn neurones following peripheral inflammation. *J Physiol* **537**, 115–123.

Guo W, Wei F, Zou S, Robbins MT, Sugiyo S, Ikeda T, Tu JC, Worley PF, Dubner R & Ren K (2004). Group I metabotropic glutamate receptor NMDA receptor coupling and signaling cascade mediate spinal dorsal horn NMDA receptor 2B tyrosine phosphorylation associated with inflammatory hyperalgesia. *J Neurosci* **24**, 9161–9173.

Guo W, Zou S, Guan Y, Ikeda T, Tal M, Dubner R & Ren K (2002). Tyrosine phosphorylation of the NR2B subunit of the NMDA receptor in the spinal cord during the development and maintenance of inflammatory hyperalgesia. *J Neurosci* **22**, 6208–6217.

Han ZS, Zhang ET & Craig AD (1998). Nociceptive and thermoreceptive lamina I neurons are anatomically distinct. *Nat Neurosci* **1**, 218–225.

Hartmann B, Ahmadi S, Heppenstall PA, Lewin GR, Schott C, Borchardt T, Seeburg PH, Zeilhofer HU, Sprengel R & Kuner R (2004). The AMPA receptor subunits GluR-A and GluR-B reciprocally modulate spinal synaptic plasticity and inflammatory pain. *Neuron* **44**, 637–650.

Iadarola MJ, Douglass J, Civelli O & Naranjo JR (1988). Differential activation of spinal cord dynorphin and enkephalin neurons during hyperalgesia: evidence using cDNA hybridization. *Brain Res* **455**, 205–212.

Ikeda H, Heinke B, Ruscheweyh R & Sandkuhler J (2003). Synaptic plasticity in spinal lamina I projection neurons that mediate hyperalgesia. *Science* **299**, 1237–1240.

Ikeda H, Stark J, Fischer H, Wagner M, Drdla R, Jager T & Sandkuhler J (2006). Synaptic amplifier of inflammatory pain in the spinal dorsal horn. *Science* **312**, 1659–1662.

Isaac JT (2003). Postsynaptic silent synapses: evidence and mechanisms. *Neuropharmacology* **45**, 450–460.

Jung SJ, Kim YS, Kim DK, Kim J & Kim SJ (2005). Long-term potentiation of silent synapses in substantia gelatinosa neurons. *Neuroreport* **16**, 961–965.

Koike M, Iino M & Ozawa S (1997). Blocking effect of 1-naphthyl acetyl spermine on Ca^{2+}-permeable AMPA receptors in cultured rat hippocampal neurons. *Neurosci Res* **29**, 27–36.

Kyrozis A, Goldstein PA, Heath MJ & MacDermott AB (1995). Calcium entry through a subpopulation of AMPA receptors desensitized neighbouring NMDA receptors in rat dorsal horn neurons. *J Physiol* **485**, 373–381.

Li P & Zhuo M (1998). Silent glutamatergic synapses and nociception in mammalian spinal cord. *Nature* **393**, 695–698.

Liu SQ & Cull-Candy SG (2000). Synaptic activity at calcium-permeable AMPA receptors induces a switch in receptor subtype. *Nature* **405**, 454–458.

Mantyh PW, Rogers SD, Honore P, Allen BJ, Ghilardi JR, Li J, Daughters RS, Lappi DA, Wiley RG & Simone DA (1997). Inhibition of hyperalgesia by ablation of lamina I spinal neurons expressing the substance P receptor. *Science* **278**, 275–279.

Monyer H, Burnashev N, Laurie DJ, Sakmann B & Seeburg PH (1994). Developmental and regional expression in the rat brain and functional properties of four NMDA receptors. *Neuron* **12**, 529–540.

Nagy GG, Al-Ayyan M, Andrew D, Fukaya M, Watanabe M & Todd AJ (2004*a*). Widespread expression of the AMPA receptor GluR2 subunit at glutamatergic synapses in the rat spinal cord and phosphorylation of GluR1 in response to noxious stimulation revealed with an antigen-unmasking method. *J Neurosci* **24**, 5766–5777.

Nagy GG, Watanabe M, Fukaya M & Todd AJ (2004*b*). Synaptic distribution of the NR1, NR2A and NR2B subunits of the N-methyl-d-aspartate receptor in the rat lumbar spinal cord revealed with an antigen-unmasking technique. *Eur J Neurosci* **20**, 3301–3312.

Nichols ML, Allen BJ, Rogers SD, Ghilardi JR, Honore P, Luger NM, Finke MP, Li J, Lappi DA, Simone DA & Mantyh PW (1999). Transmission of chronic nociception by spinal neurons expressing the substance P receptor. *Science* **286**, 1558–1561.

Oliet SH, Malenka RC & Nicoll RA (1996). Bidirectional control of quantal size by synaptic activity in the hippocampus. *Science* **271**, 1294–1297.

Plant K, Pelkey KA, Bortolotto ZA, Morita D, Terashima A, McBain CJ, Collingridge GL & Isaac JT (2006). Transient incorporation of native GluR2-lacking AMPA receptors during hippocampal long-term potentiation. *Nat Neurosci* **9**, 602–604.

Rudhard Y, Kneussel M, Nassar MA, Rast GF, Annala AJ, Chen PE, Tigaret CM, Dean I, Roes J, Gibb AJ, Hunt SP & Schoepfer R (2003). Absence of Whisker-related pattern formation in mice with NMDA receptors lacking coincidence detection properties and calcium signaling. *J Neurosci* **23**, 2323–2332.

Rycroft BK, Vikman KS & Christie MJ (2007). Inflammation reduces the contribution of N-type calcium channels to primary afferent synaptic transmission onto NK1 receptor-positive lamina I neurons in the rat dorsal horn. *J Physiol* **580**, 883–894.

Sasaki YF, Rothe T, Premkumar LS, Das S, Cui J, Talantova MV, Wong HK, Gong X, Chan SF, Zhang D, Nakanishi N, Sucher NJ & Lipton SA (2002). Characterization and comparison of the NR3A subunit of the NMDA receptor in recombinant systems and primary cortical neurons. *J Neurophysiol* **87**, 2052–2063.

Schramm NL, Egli RE & Winder DG (2002). LTP in the mouse nucleus accumbens is developmentally regulated. *Synapse* **45**, 213–219.

Sorkin LS, Yaksh TL & Doom CM (2001). Pain models display differential sensitivity to Ca^{2+}-permeable non-NMDA glutamate receptor antagonists. *Anesthesiology* **95**, 965–973.

Soto D, Coombs ID, Kelly L, Farrant M & Cull-Candy SG (2007). Stargazin attenuates intracellular polyamine block of calcium-permeable AMPA receptors. *Nat Neurosci* **10**, 1260–1267.

Thiagarajan TC, Lindskog M & Tsien RW (2005). Adaptation to synaptic inactivity in hippocampal neurons. *Neuron* **47**, 725–737.

Todd AJ, Spike RC & Polgar E (1998). A quantitative study of neurons which express neurokinin-1 or somatostatin sst2a receptor in rat spinal dorsal horn. *Neuroscience* **85**, 459–473.

Tölle TR, Berthele A, Zieglgansberger W, Seeburg PH & Wisden W (1993). The differential expression of 16 NMDA and non-NMDA receptor subunits in the rat spinal cord and in periaqueductal gray. *J Neurosci* **13**, 5009–5028.

Tong CK & MacDermott AB (2006). Both Ca^{2+}-permeable and -impermeable AMPA receptors contribute to primary synaptic drive onto rat dorsal horn neurons. *J Physiol* **575**, 133–144.

Tong G, Shepherd D & Jahr CE (1995). Synaptic desensitization of NMDA receptors by calcineurin. *Science* **267**, 1510–1512.

Wyllie DJ, Behe P & Colquhoun D (1998). Single-channel activations and concentration jumps: comparison of recombinant NR1a/NR2A and NR1a/NR2D NMDA receptors. *J Physiol* **510**, 1–18.

Wyllie DJ, Behe P, Nassar M, Schopfer R & Colquhoun D (1996). Single-channel currents from recombinant NMDA NR1a/NR2D receptors expressed in Xenopus oocytes. *Proc Biol Sci* **263**, 1079–1086.

Acknowledgements

This work was supported by the National Health and Medical Research Council of Australia (Program Grant 351446, Fellowship 253799 to M.J.C.) and NSW Spinal Cord Injury and Other Neurological Conditions Program Grant (R1PG5). K.S.V. was also supported by the Australian and New Zealand College of Anaesthetists (05/009) and the Swedish Brain Foundation.